

Author's Accepted Manuscript

Fiber-optic Confocal Laser Endomicroscopy of Small Renal Masses: Towards Real-time Optical Diagnostic Biopsy

Li-Ming Su , Jennifer Kuo , Robert W. Allan , Joseph C. Liao , Kellie L. Ritari , Patrick E. Tomeny , Christopher M. Carter



PII: S0022-5347(15)04704-7
DOI: [10.1016/j.juro.2015.07.115](https://doi.org/10.1016/j.juro.2015.07.115)
Reference: JURO 12883

To appear in: *The Journal of Urology*
Accepted Date: 7 July 2015

Please cite this article as: Su LM, Kuo J, Allan RW, Liao JC, Ritari KL, Tomeny PE, Carter CM, Fiber-optic Confocal Laser Endomicroscopy of Small Renal Masses: Towards Real-time Optical Diagnostic Biopsy, *The Journal of Urology*® (2015), doi: 10.1016/j.juro.2015.07.115.

DISCLAIMER: This is a PDF file of an unedited manuscript that has been accepted for publication. As a service to our subscribers we are providing this early version of the article. The paper will be copy edited and typeset, and proof will be reviewed before it is published in its final form. Please note that during the production process errors may be discovered which could affect the content, and all legal disclaimers that apply to The Journal pertain.

Embargo Policy

All article content is under embargo until uncorrected proof of the article becomes available online.

We will provide journalists and editors with full-text copies of the articles in question prior to the embargo date so that stories can be adequately researched and written. The standard embargo time is 12:01 AM ET on that date. Questions regarding embargo should be directed to jumedia@elsevier.com.

Fiber-optic Confocal Laser Endomicroscopy of Small Renal Masses: Towards Real-time Optical Diagnostic Biopsy

Li-Ming Su¹, Jennifer Kuo¹, Robert W. Allan², Joseph C. Liao³, Kellie L. Ritari¹, Patrick E. Tomeny¹, and Christopher M. Carter²

¹Departments of Urology, University of Florida College of Medicine, Gainesville, FL

²Department of Surgical Pathology, University of Florida College of Medicine, Gainesville, FL

³Department of Urology, Stanford University School of Medicine, Stanford, CA

Running Title: Confocal laser endomicroscopy of small renal masses

Key Words: confocal microscopy; small renal masses; optical biopsy

ABSTRACT

Introduction: The incidental detection of small renal masses is on the rise. However, not all require aggressive treatments as up to 20% are benign and the majority of malignant tumors harbor indolent features. Improved preoperative diagnostics are needed to differentiate tumors requiring aggressive treatment from those more suitable for surveillance. We evaluated and compared confocal laser endomicroscopy (CLE) with standard histopathology in *ex vivo* human kidney tumors as a proof-of-principle towards diagnostic optical biopsy.

Methods: Patients with solitary small renal masses scheduled for partial or radical nephrectomy were enrolled in the study. Two kidneys were infused with fluorescein via intraoperative intravenous injection, and 18 tumors were bathed *ex vivo* in dilute fluorescein prior to confocal imaging. A 2.6 mm CLE probe was used to image tumors and surrounding parenchyma from external and en face surfaces after specimen bisection. CLE images were compared to standard H&E analysis of corresponding areas.

Results: *Ex vivo* CLE imaging revealed normal renal structures that correlated well with histology. Tumor tissue was readily distinguishable from normal parenchyma, demonstrating features unique to benign and malignant tumor subtypes. Topical fluorescein administration provided more consistent CLE imaging than the intravenous route. Additionally, en face tumor imaging was superior to external imaging.

Conclusion: We report the first feasibility study using CLE to evaluate small renal masses *ex vivo* and provide a preliminary atlas of images from various renal neoplasms with corresponding histology. These findings serve as an initial and promising step towards real-time, diagnostic optical biopsy of small renal masses.

Introduction:

The incidental detection of small (<4 cm) solid renal masses (SRM) has steadily increased due to the widespread use of ultrasonography (US), cross-sectional computed tomography (CT), and magnetic resonance imaging (MRI). Unfortunately, these imaging modalities are imprecise in discriminating between benign and malignant tumors, not to mention the various subtypes and grades of malignant tumors. Therefore, they provide the urologist with limited guidance as to the most appropriate therapy based on tumor type. This is especially germane given the expanded treatment options for SRMs, which include active surveillance and thermal ablation, in addition to radical and nephron-sparing surgery. Furthermore, the field has gained a greater appreciation for the genetic heterogeneity of renal cell carcinoma, prompting the development of new targeted medical therapies tailored to specific molecular pathways and renal tumor subtypes.¹ This leads to a clinical decision-making paradigm that is currently not optimal. For example, surgical resection for many tumors may be considered overly aggressive or even unnecessary, especially in medically frail patients, given that up to 20% of resected SRMs are found to be benign on histopathology and an additional 60% of malignant tumors are found to harbor indolent features.^{2,3} Taken together, these observations

suggest that our therapeutic interventions have advanced faster than our diagnostic modalities, highlighting the clear need for improved diagnostic testing that can properly match the biological aggressiveness of a tumor with the most appropriate treatment option.

Percutaneous diagnostic renal biopsy has historically been used to address this problem, but has been limited in use due to the concern of diagnostic inaccuracy and the fear of complications such as bleeding and tumor seeding along the needle tract.⁴ Several novel optical imaging modalities have recently been under development towards the goal of “optical biopsy.” These approaches hope to use optical techniques to harvest diagnostic and prognostic information that has previously only been available from final histopathology. Optical imaging encompasses a variety of technologies that generate data based on the unique absorption, scattering, reflectance, and fluorescence profiles produced upon light interaction with various tissue, structural, and cellular components. In some cases, this data can be displayed as an image output. Technologies most pertinent to urology include photodynamic diagnosis (PDD), narrow-band imaging (NBI), and optical coherence tomography (OCT). PDD and NBI have been used as enhancements to standard white light cystoscopy (WLC) for identification of bladder neoplasms, and OCT has been used in the evaluation of both bladder and kidney neoplasms.⁵⁻¹²

Confocal microscopy (CM) is a well-established optical imaging technology in the basic science field that provides high resolution, real-time images of tissues on a microscopic level. This technology requires the administration of a fluorescent dye to augment the resolution of cellular and tissue architecture from surrounding blood supply and connective tissue. CM is based upon laser excitation of tissues with acquisition of backscattered fluorescent light through a pinhole aperture that rejects light from out-of-focus planes, thus providing a clear, in-focus image of a very thin section of tissue. Miniaturization of instruments has led to the development of a fiber-optic confocal delivery system that can be passed through the working channel of standard endoscopes for *in vivo* imaging, now referred to as confocal laser endomicroscopy (CLE).¹³ CLE has been approved for use in the fields of gastroenterology and pulmonology for evaluation of Barrett’s esophagus, cystic fibrosis, gastric cancer and others.¹⁴⁻¹⁶ For gastric cancer, CLE demonstrated significantly higher diagnostic accuracy when compared with conventional endoscopic biopsies in differentiating gastric adenomas from adenocarcinomas (94.2% vs 85.7%, $p=0.031$).¹⁷

The U.S. Food & Drug Administration has also approved the endoscopic application of CLE in the field of urology. To date, studies of CLE imaging within the field of urology have been predominantly focused on urothelial carcinoma. Sonn *et al.* have demonstrated the ability of CLE to adequately visualize differences between normal urothelial mucosa and tumor tissue within the bladder.^{18,19} In addition, CLE images representing different tissue types within the genitourinary tract have been compiled into an imaging atlas, establishing a preliminary set of diagnostic criteria for future studies.²⁰ Until now, CM imaging of kidney tissue has been limited to animal models using bench-top confocal microscopes.²¹ Campo-Ruiz and colleagues demonstrated in a murine model that CM

imaging of renal tubules, glomeruli, and interstitium correlated highly with hematoxylin and eosin histology on a structural and cellular level.

Building upon these aforementioned studies, we evaluated the utility of CLE imaging of *ex vivo* human renal tumors following surgical excision as compared to standard histopathology as a proof-of-principle study towards the development of diagnostic optical biopsy.

Methods:

Patient Enrollment. Following protocol approval by the Institutional Review Board at the University of Florida, a total of 20 patients with solitary small renal tumors scheduled for partial (n=13) or radical (n=7) nephrectomy were enrolled in this study between October 2013 and December 2014 (Table 1). Informed consent for the study was obtained from all patients prior to surgery. All surgeries and CLE imaging were performed by a single surgeon.

Fluorescein Administration. In the first two study patients, five mL of 10% fluorescein (Alcon Laboratories, Inc., Fort Worth, TX) was administered intraoperatively by peripheral intravenous injection approximately five minutes prior to renal hilar transection in radical nephrectomy cases or renal artery clamping in partial nephrectomy cases. This was to allow for adequate kidney and tumor tissue uptake of fluorescein. After surgical resection, *ex vivo* CLE imaging of these two specimens was performed in the pathology lab following completion of the surgery. In the ensuing eighteen patients, surgically resected tumors were removed from surrounding perinephric fat and bathed *ex vivo* for five minutes in 200 mL of normal saline containing 0.0005% fluorescein for tissue staining.

Ex vivo Confocal Imaging. All specimens were rinsed with 250 mL normal saline to remove excess fluorescein prior to CLE imaging. The CLE imaging system used (Cellvizio, Mauna Kea Technologies Inc., Suwanee, GA) was equipped with a laser scanning unit (488 nm excitation wavelength), 2.6 mm fiber-optic probe and a desktop computer with image acquisition and processing software. The 2.6 mm probe has an image resolution of 1 μm , field of view of 240 μm and a depth of focus of 60 μm . CLE video imaging was performed on five regions of the external tumor surface and on regions of the surrounding normal parenchyma. Following this, the tumor specimen was bisected for *en face* CLE imaging on five regions of the tumor cut-surface and on regions of the surrounding normal parenchyma (Figure 1). Images were collected as video sequences at 12 frames per second and stored for later review with corresponding histopathology.

Histopathologic Analysis. Following CLE imaging, interrogated regions were carefully marked with colored dyes to ensure the same regions of tumor and normal parenchyma were biopsied for optimal imaging-histology co-registration (Figure 2). Biopsies were processed for standard pathological assessment with hematoxylin and eosin by one of two dedicated uropathologists on the study team. Representative CLE still-frame images were taken from video segments of various benign and malignant renal tumor subtypes and

compiled into a CLE atlas of images with corresponding histopathology.

Results:

CLE imaging from the first two patients who received intravenous fluorescein had suboptimal image quality that limited the ability to accurately visualize cellular architecture and structure. Subsequently, direct topical administration of fluorescein provided much improved and consistent image quality. Tissue microarchitecture could not be well visualized when imaging from the external surface of the renal capsule or tumor pseudocapsule. However, en face imaging with the probe in direct contact with tumor tissue allowed for discrimination of structures within normal renal tissue (i.e. glomeruli, tubules, sinus fat and collecting system) with excellent correlation to histology (Figure 3). For example, individual cuboidal epithelial cells highlighted by fluorescein staining of cytoplasm could be seen lining the renal tubules. The nuclei of these cells appeared dark due to poor fluorescein penetration through the nuclear membrane, as did the network of capillaries within the glomerulus. In contrast, urothelial cells of the renal pelvis and sinus fat appeared dark and were accentuated by fluorescein staining of extracellular matrix rather than cytoplasm. Tumor tissue was readily distinguished from normal parenchyma, as were features unique to benign tumor subtypes (Figure 4). Of the benign tumor subtypes, angiomyolipoma was remarkably distinctive for its characteristic fat globules that appeared as dark, spherical bodies embedded in an amorphous background of muscle and vessels. Oncocytoma demonstrated dark nests of cells delineated by fluorescein staining of intervening fibromyxoid stroma. Spindle cells could be seen in both leiomyoma and cystic nephroma tumors. However, unlike cystic nephroma, leiomyoma exhibited broad fascicles with the classic whorl-like, trabeculated pattern reminiscent of histologic findings. Although sufficient fluorescein penetration into normal renal tissue allowed for excellent imaging, poor fluorescein penetration into tumor cells, especially in malignant tumor subtypes, limited image content to mere structural outlines of tumor architecture without cellular distinction (Figure 5). As such, histologic grade could not be assessed due to limitations in CLE image quality of the nucleus as well as the small sample size. Clear cell RCC exhibited a thunder storm-like pattern, whereas, acquired cystic RCC had better fluorescein uptake that allowed for visualization of intranuclear vacuoles. Papillary RCC demonstrated characteristic papillae despite the lack of cellular detail due to poor fluorescein uptake. In addition, passing red blood cells within vascular networks were easily visualized within angiomyolipomas, clear cell RCC, and fibrovascular stalks of papillary RCC.

Discussion:

We report the first confocal laser endomicroscopic evaluation of *ex vivo* human renal tumors. Using fresh surgical specimens, we acquired real-time CLE images with resolution sufficient for visualizing microarchitecture and cellular morphology characteristic of both normal and tumor tissue. In our study, we made the following observations. First, *ex vivo* administration of topical fluorescein allowed for more consistent, uniform and superior staining of tissue specimens as compared to *in vivo* peripheral administration of intravenous fluorescein. Others have previously shown that intravenous fluorescein delivery provides excellent CLE image resolution in bladder tumors.^{18,19} Therefore we believe that our observation was likely due to improper dosing

and timing between administration and imaging. Additionally, significant renal blood flow through the human kidney in conjunction with the amount of time required to resect and deliver the tumor specimen from the body (45-60 minutes) likely allowed dye to transit from renal tissues before *ex vivo* CLE imaging could be completed, resulting in poor contrast between cellular structures and surrounding interstitium. A higher dose may have been required to deliver sufficient volume of dye from the systemic circulation to the kidney and tumor. Second, en face CLE imaging of bisected specimens was superior to external tumor surface imaging likely due to the limited depth of penetration of CLE (i.e. 60 μm). The presence of tumor pseudocapsule was enough to prevent visualization of subcapsular cellular and structural detail. As with all light-based optical technologies, there is an inherent trade-off between depth of light penetration and image resolution. Third, CLE provided excellent discrimination of various anatomic components within normal renal tissue, including tubules, glomeruli, collecting system, and perinephric fat analogous to histopathology. Fourth, CLE imaging could easily discern between tumor tissue and normal tissue. However, malignant tumor subtypes were not as well delineated as benign tumor subtypes due to limited fluorescein penetration into malignant cells although some tumor structures were still striking such as the papillae in papillary renal cell carcinoma. There is evidence that besides passive diffusion in accordance to pH partition theory there are also select isoforms of pH-dependent monocarboxylic acid transporters (MCTs) involved in the cellular uptake of fluorescein. The kidney expresses several MCT isoforms in distinct cellular distributions such that cells in the proximal tubules express different isoforms from those in the distal tubules, which may account for differential fluorescein uptake among normal cells.²² Additionally, decreased fluorescein uptake in malignant cells may be explained by modified expression of MCTs or alterations in intra- and extracellular pH secondary to pathologic metabolic remodeling.²³ Potential alternatives include the use of fluorescein conjugated antibodies or other fluorescence probes that may target and penetrate cellular compartments of tumor cells as compared to predominately interstitial spaces with fluorescein. Another important point of consideration in CLE imaging is that real-time acquisition of video sequences provides more than a single field of view (Video 1). The single still-images isolated from CLE video sequences do not fully capture the overall gestalt and patterns of cellular and tumor architecture that aid in the differentiation of tumor subtypes.

While promising, our *ex vivo* pilot study has several limitations apropos to the utility of CLE as a preoperative, diagnostic optical biopsy tool for SRMs. First, an ideal optical biopsy tool would potentially replace the need for percutaneous needle biopsy by providing immediate, real-time data in the *in vivo* setting. In our study, we used a probe size that obviates the percutaneous application of CLE technology. A 2.6 mm diameter probe was favored over another available smaller diameter (0.85 mm) probe for its higher spatial resolution, 1 μm and 3.5 μm respectively. The smaller diameter probe fits within standard 19 gauge biopsy needles, but the image quality is inferior. Also limiting the *in vivo* application of CLE was our reliance on topical fluorescein administration as opposed to the intravenous route. Although tangential from our goal of preoperative diagnosis, the timing and dosing of intravenous fluorescein administration could be further investigated and refined to allow for future intraoperative applications such as inspecting tumor beds or partial nephrectomy specimens for positive surgical margins. Prior work in bladder

tumors suggest that intravenous fluorescein allows for adequate imaging within 1-2 minutes and up to 30 minutes following injection.²⁴ Second, an ideal optical biopsy tool would provide adequate information through superficial contact that does not penetrate the actual surface of the tumor, thus avoiding the risk of tumor cell spillage. However, we observed a limited depth of light penetration when imaging from the external surface of the renal tumor. Any overlying adipose tissue, normal parenchyma, or even tumor pseudocapsule hindered image penetration and significantly deterred visualization of underlying tissue, rendering images inadequate for purposes of tissue characterization. Although tumor penetration with a CLE probe does not circumvent the concern of tumor spillage akin to standard biopsy, it does have the advantage of live, continuous acquisition of images unlike the static result from needle biopsy. Also, tumor penetration may have utility in improving the yield of a standard biopsy by providing real-time feedback (e.g. avoiding acellular regions).

Despite these limitations, improvements in CLE and other fiberoptic-based technologies are worthy of pursuit in order to enhance the armamentarium of diagnostic imaging modalities used in the field of urology as well as other fields of medicine. Studies have demonstrated the potential of CLE as an adjunct to white light cystoscopy in bladder cancer.^{13,14} As a hollow organ, the bladder offers a direct route for *in vivo* topical fluorescein administration and unhindered imaging of tumor tissue. In our attempt to extend the diagnostic spectrum of CLE to SRMs, we were confronted by significant obstacles intrinsic to the imaging process of a solid organ and tumor. However, these obstacles define a path for further development in CLE and other optical imaging technologies that will improve light penetration while maintaining the capacity for high-resolution imaging. More significantly, our study accomplished an important goal in establishing a baseline set of CLE images of normal renal tissue and benign and malignant tumor subtypes for future clinical urologic research.

Conclusions:

We report the first feasibility study of using CLE optical biopsy for the *ex vivo* evaluation of solid renal tumors. Additionally, we provide a preliminary atlas of confocal images from various renal neoplasms with corresponding histology. The real-time procurement of information using technologies such as CLE may provide instantaneous and actionable data that improves patient counseling and clinical decision-making. Beyond the field of urology, progress in this area may eventually revolutionize how pathologists and radiologists approach and image renal tumors in the future.

Source of Funding: Departmental

Table 1. Patient demographics, surgical type and tumor characteristics. RCC, renal cell carcinoma.

Figure 1. En face confocal imaging of renal tumor with confocal 488 nm laser light transmitted through a 2.6 mm fiber-optic probe.

Figure 2. Confocal laser endomicroscopy imaged tumor regions marked with colored dyes for directed biopsy for histopathology.

Figure 3. Normal renal tissues. Comparison of H&E and en face confocal endomicroscopic images of normal glomerulus and tubules (A,B), renal pyramid (C,D), renal pelvis (E,F), and sinus fat (G,H).

Figure 4. Benign renal tumors. Comparison of H&E and en face confocal endomicroscopic images of angiomyolipoma (A,B), oncocytoma (C,D), cystic nephroma (E,F), and leiomyoma (G,H).

Figure 5. Malignant renal tumors. Comparison of H&E and en face confocal endomicroscopic images of clear cell renal cell carcinoma (A,B), papillary renal cell carcinoma (C,D), and acquired cystic renal cell carcinoma (E,F).

References:

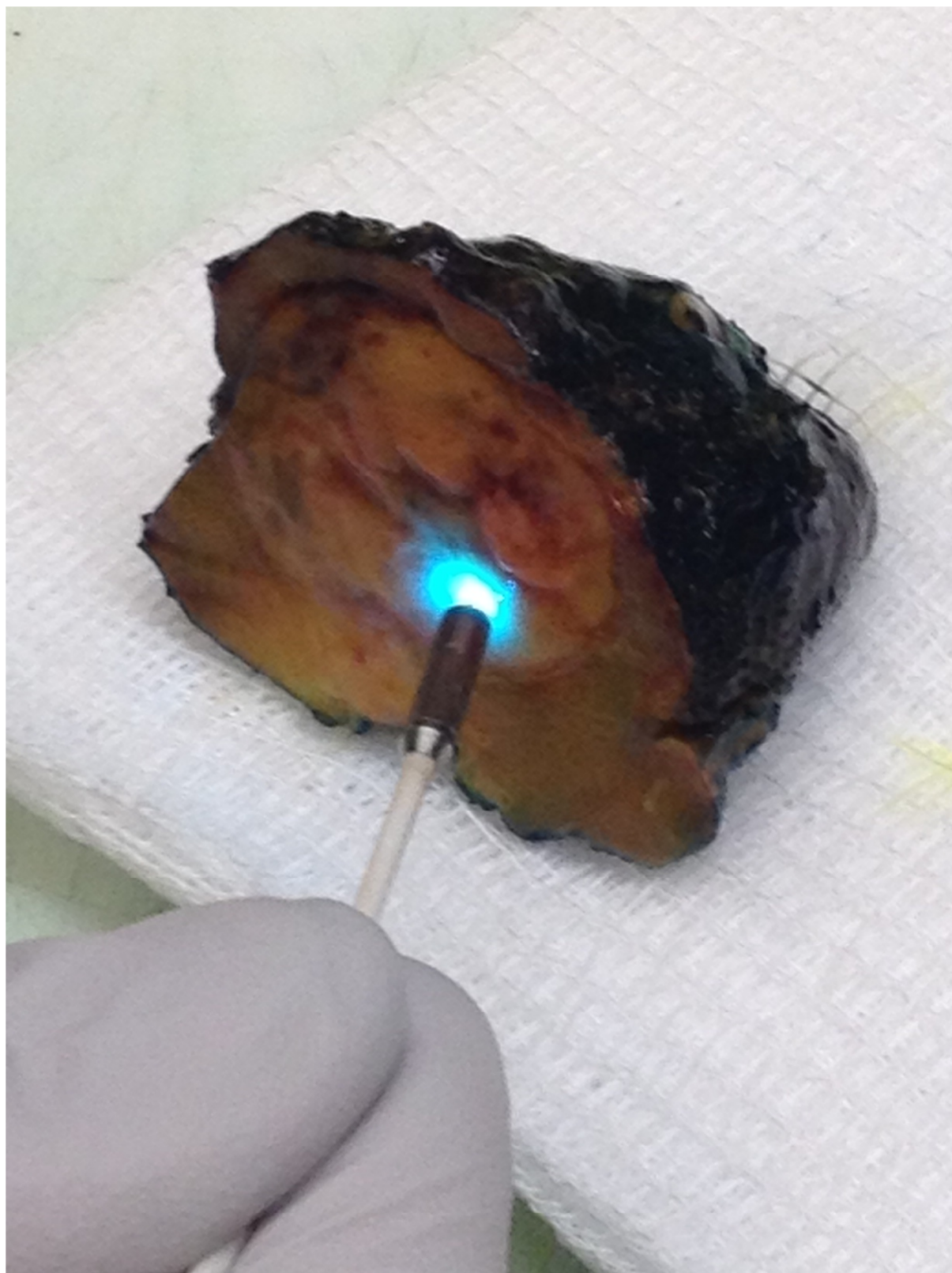
- [1] W. Linehan, R. Srinivasan, L. Schmidt, The genetic basis of kidney cancer: a metabolic disease, *Nat Rev Urol.* 7 (2010) 277-285. doi:10.1038/nrurol.2010.47.
- [2] B. Lane, D. Babineau, M. Kattan et al., A Preoperative Prognostic Nomogram for Solid Enhancing Renal Tumors 7 cm or Less Amenable to Partial Nephrectomy, *J Urol.* 178 (2007) 429-434. doi:10.1016/j.juro.2007.03.106.
- [3] A. Kutikov, M. Smaldone, B. Egleston et al., Anatomic Features of Enhancing Renal Masses Predict Malignant and High-Grade Pathology: A Preoperative Nomogram Using the RENAL Nephrometry Score, *Eur Urol.* 60 (2011) 241-248. doi:10.1016/j.eururo.2011.03.029.
- [4] B. Lane, M. Samplaski, B. Herts et al., Renal mass biopsy--a renaissance? *J Urol.* 179 (2008) 20-27. doi:10.1016/j.juro.2007.08.124
- [5] A. Lapini, A. Minervini, A. Masala et al., A comparison of hexaminolevulinate (Hexvix®) fluorescence cystoscopy and white-light cystoscopy for detection of bladder cancer: results of the HeRo observational study, *Surg Endosc.* 26 (2012) 3634-3641. doi:10.1007/s00464-012-2387-0.
- [6] M. Rink, M. Babjuk, J. Catto et al., Hexyl Aminolevulinate-Guided Fluorescence Cystoscopy in the Diagnosis and Follow-up of Patients with Non-Muscle-invasive Bladder Cancer: A Critical Review of the Current Literature, *Eur Urol.* 64 (2013) 624-638. doi:10.1016/j.eururo.2013.07.007.
- [7] E. Cauberg, S. Kloen, M. Visser et al., Narrow Band Imaging Cystoscopy Improves the Detection of Non-muscle-invasive Bladder Cancer, *Urology.* 76 (2010) 658-663. doi:10.1016/j.urology.2009.11.075.
- [8] H. Lee, C. Zhou, D. Cohen et al., Integrated optical coherence tomography and optical coherence microscopy imaging of ex vivo human renal tissues, *J Urol.* 182 (2012) 691-699. doi:10.1016/j.juro.2011.09.149.
- [9] K. Barwari, D. de Bruin, D. Faber et al., Differentiation between normal renal tissue and renal tumours using functional optical coherence tomography: a phase I in vivo human study, *BJU Int.* 110 (2012) 415-420. doi:10.1111/j.1464-410X.2012.11197.x.
- [10] M. Manyak, N. Gladkova, J. Makari et al., Evaluation of superficial bladder transitional-cell carcinoma by optical coherence tomography, *J Endourol.* 19 (2005) 570-574.
- [11] S. Lerner, A. Goh, N. Tresser et al., Optical coherence tomography as an adjunct to white light cystoscopy for intravesical real-time imaging and staging of bladder cancer, *Urology.* 72 (2008) 133-137.

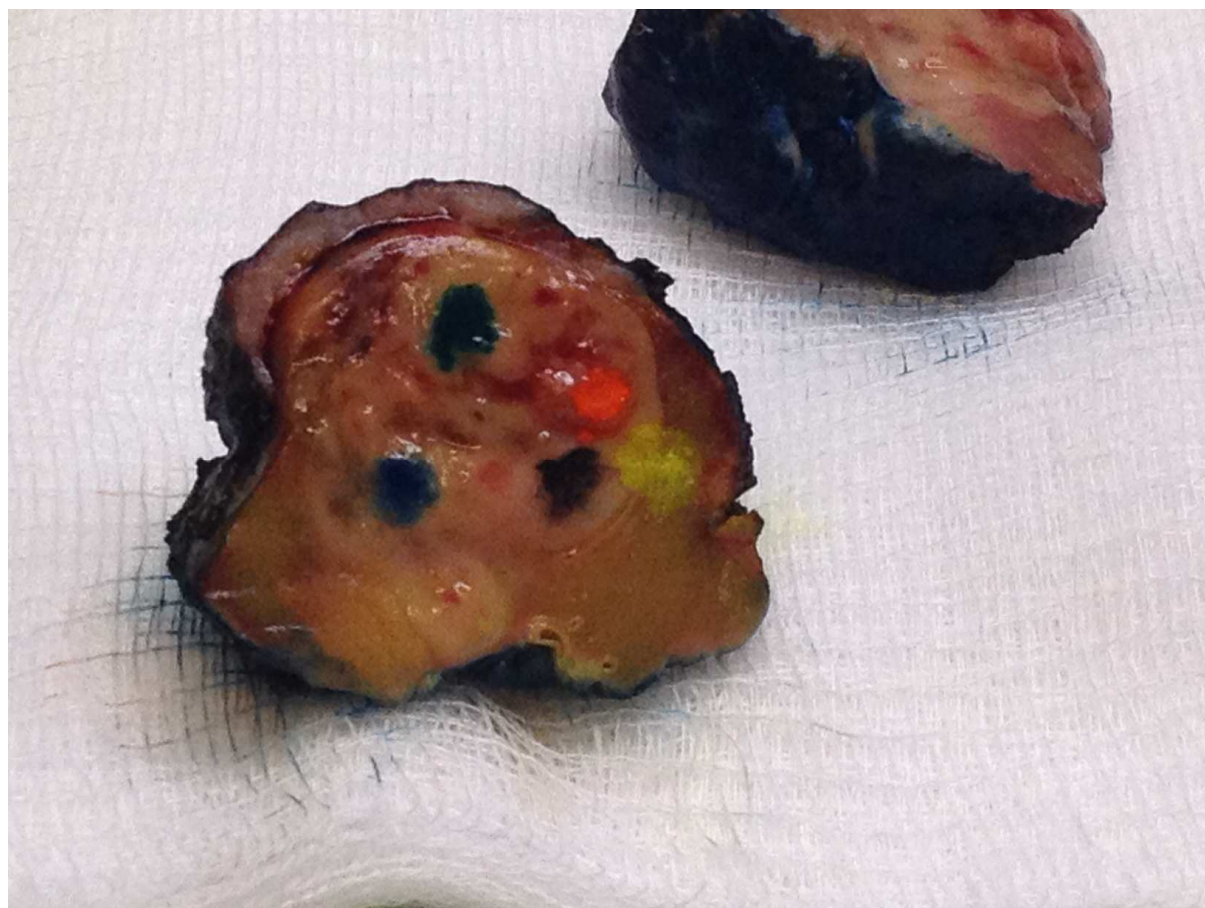
- [12] B. Hermes, F. Spöler, A. Naami et al., Visualization of the basement membrane zone of the bladder by optical coherence tomography: Feasibility of noninvasive evaluation of tumor invasion, *Urology*. 72 (2008) 677–681.
- [13] F. Helmchen, Miniaturization of Fluorescence Microscopes Using Fiber Optics, *Exp Physiol*. 87 (2002) 737-745. DOI: 10.1113/eph8702478
- [14] K. Banno, Y. Niwa, R. Miyahara et al., Confocal endomicroscopy for phenotypic diagnosis of gastric cancer, *J Gastroenterol Hepatol*. 25 (2010) 712-718. doi:10.1111/j.1440-1746.2009.06169.x.
- [15] L. Thiberville, M. Salaun, S. Lachkar et al., Human in vivo fluorescence microimaging of the alveolar ducts and sacs during bronchoscopy, *Eur Respir J*. 33 (2009) 974-985. doi:10.1183/09031936.00083708.
- [16] T. Wang, S. Friedland, P. Sahbaie et al., Functional Imaging of Colonic Mucosa With a Fibered Confocal Microscope for Real-Time In Vivo Pathology, *Clin Gastroenterol And Hepatol*. 5 (2007) 1300-1305. doi:10.1016/j.cgh.2007.07.013.
- [17] S. Jeon, W. Cho, S. Jin et al., Optical biopsies by confocal endomicroscopy prevent additive endoscopic biopsies before endoscopic submucosal dissection in gastric epithelial neoplasias: a prospective, comparative study, *Gastrointest Endos*. 74 (2011) 772-780. doi:10.1016/j.gie.2011.05.005.
- [18] G. Sonn, S. Jones, T. Tarin et al., Optical Biopsy of Human Bladder Neoplasia With In Vivo Confocal Laser Endomicroscopy, *J Urol*. 182 (2009) 1299-1305. doi:10.1016/j.juro.2009.06.039.
- [19] G. Sonn, K. Mach, K. Jensen et al., Fibered Confocal Microscopy of Bladder Tumors: An ex vivo Study, *J Endourol*. 23 (2009) 197-202. doi:10.1089/end.2008.0524.
- [20] K. Wu, J. Liu, W. Adams et al., Dynamic Real-time Microscopy of the Urinary Tract Using Confocal Laser Endomicroscopy, *Urology*. 78 (2011) 225-231. doi:10.1016/j.urology.2011.02.057.
- [21] V. Campo-Ruiz, G. Lauwers, R. Anderson et al., Novel Virtual Biopsy of the Kidney With Near Infrared, Reflectance Confocal Microscopy, *J Urol*. 175 (2006) 327-336. doi:10.1097/00005392-200601000-00116.
- [22] H. Becker, N. Mohebbi, A. Perna et al., Localization of members of MCT monocarboxylate transporter family Slc16 in the kidney and regulation during metabolic acidosis, *Am J Physiol Renal Physiol*. 299 (2010) 141-154. doi:10.1152/ajprenal.00488.2009.

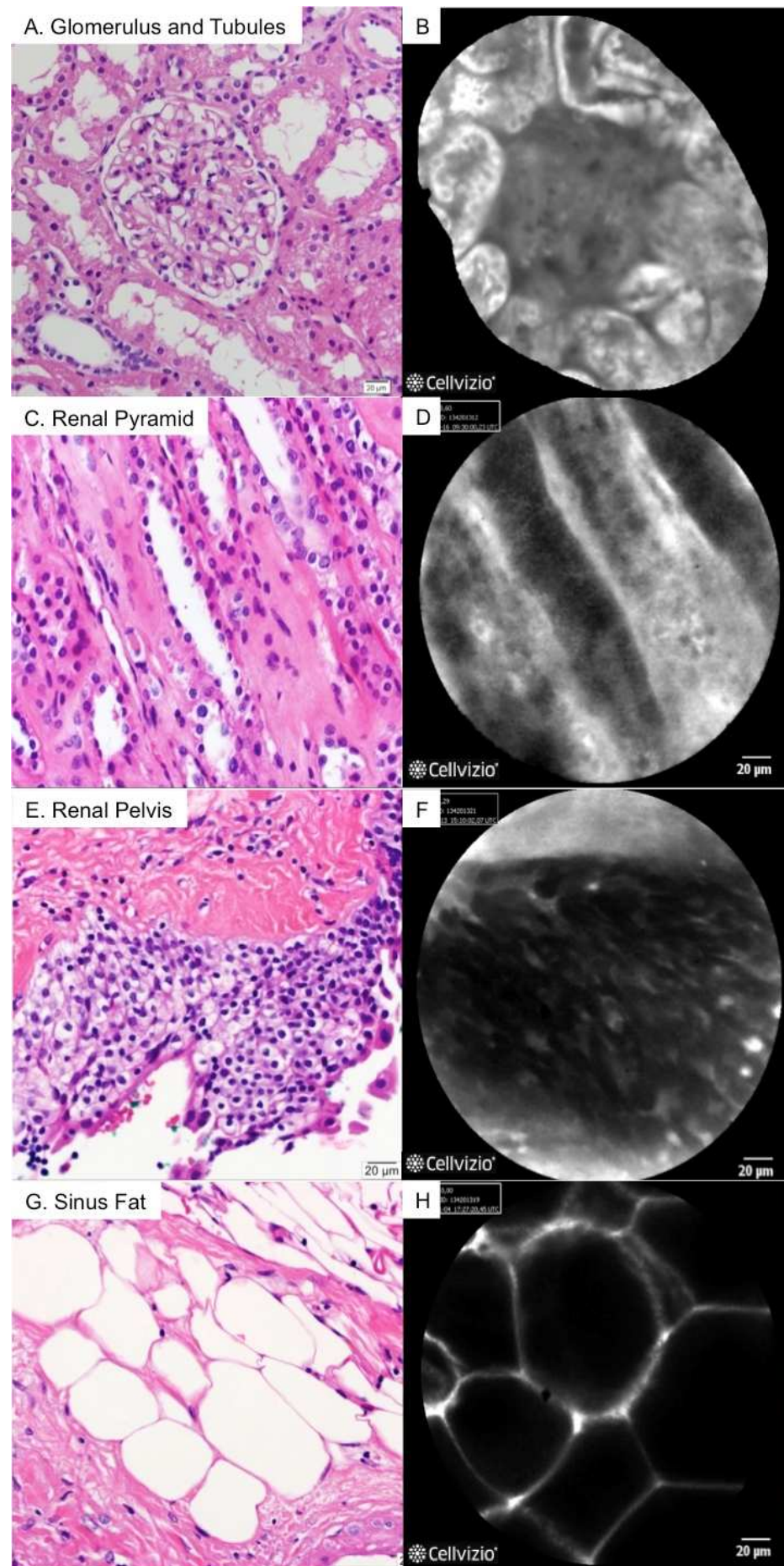
[23] K. Berginc, S. Zakelj, L. Levstik et al., Fluorescein transport properties across artificial lipid membranes, Caco-2 cell monolayers and rat jejunum, *Eur J Pharm Biopharm.* 66 (2007) 281-285.

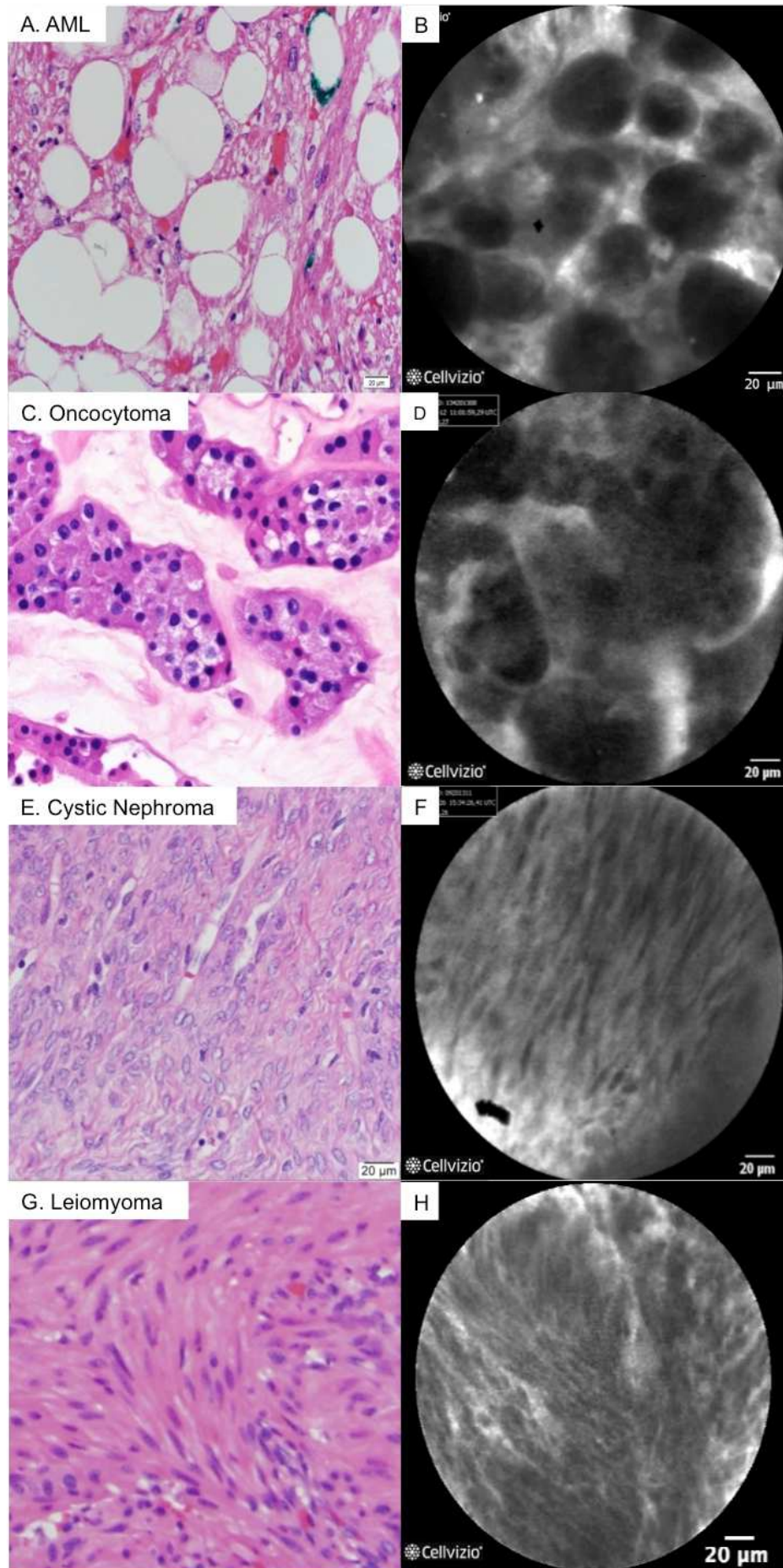
[24] T. Chang, J. Liu, J. Liao, Probe-based confocal laser endomicroscopy of the urinary tract: the technique. *J Vis Exp.* 71 (2013) 4409. doi: 10.3791/4409

Age	Gender	Tumor Size (cm)	Type of Nephrectomy	Pathology	Histologic Grade	Route of Fluorescein Administration
63	M	6.5	Radical	Oncocytoma	N/A	Intravenous
65	M	5.8	Radical	Clear cell RCC	2	Intravenous
53	M	5.0	Partial	Clear cell RCC	2	Topical
37	F	2.1	Partial	Leiomyoma	N/A	Topical
61	F	3.4	Partial	Clear cell RCC	3	Topical
83	M	4.2	Radical	Oncocytoma	N/A	Topical
55	F	3.5	Partial	Papillary RCC	2	Topical
28	M	2.2	Partial	Clear cell RCC	2	Topical
63	F	5.5	Partial	Cystic nephroma	N/A	Topical
69	M	2.0	Partial	Clear cell RCC	2	Topical
89	M	6.5	Radical	Clear cell RCC	2	Topical
62	M	1.7	Radical	Acquired cystic RCC	2 with focal areas of 3	Topical
73	M	2.5	Partial	Clear cell RCC	3	Topical
68	F	4.4	Partial	Angiomyolipoma	N/A	Topical
66	F	4.6	Radical	Clear cell RCC	2	Topical
43	M	4.2	Partial	Papillary RCC	2	Topical
80	M	2.5	Partial	Chromophobe RCC	2 with focal areas of 3	Topical
47	F	2.7	Partial	Clear cell RCC	2	Topical
82	M	5.5	Radical	Oncocytoma	N/A	Topical
53	M	1.2	Partial	Clear cell RCC	2	Topical

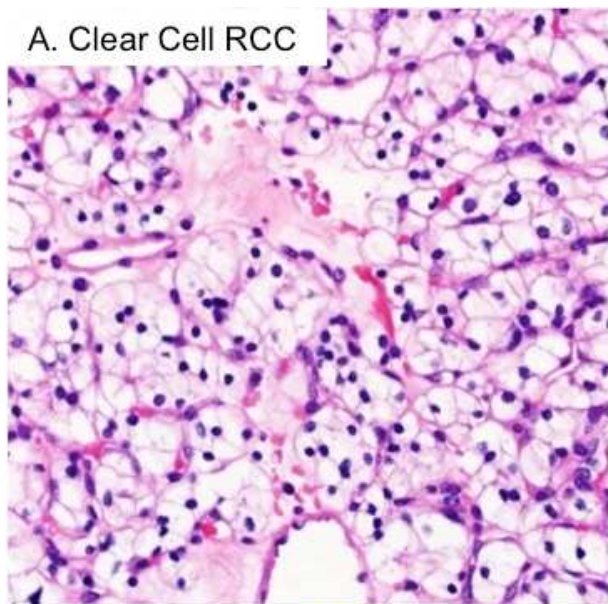




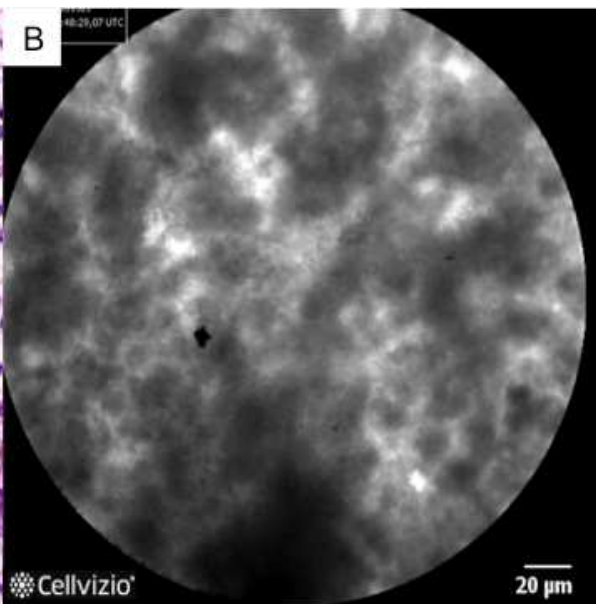




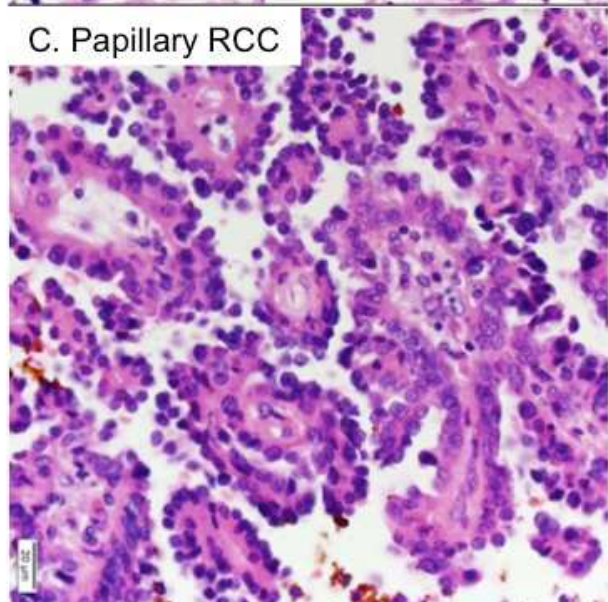
A. Clear Cell RCC



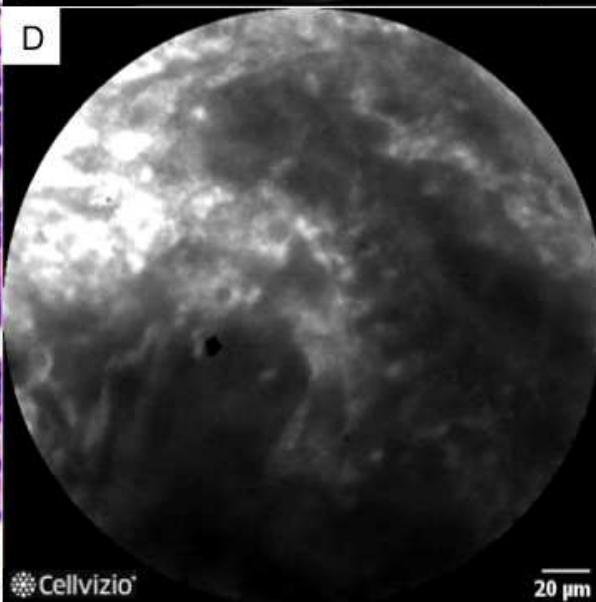
B



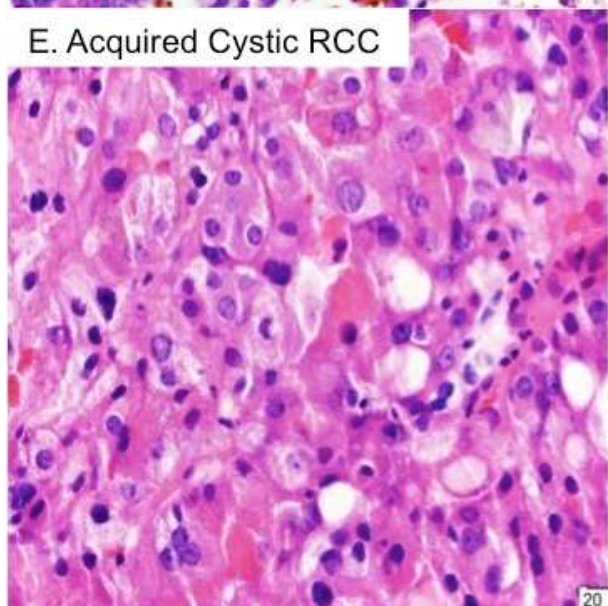
C. Papillary RCC



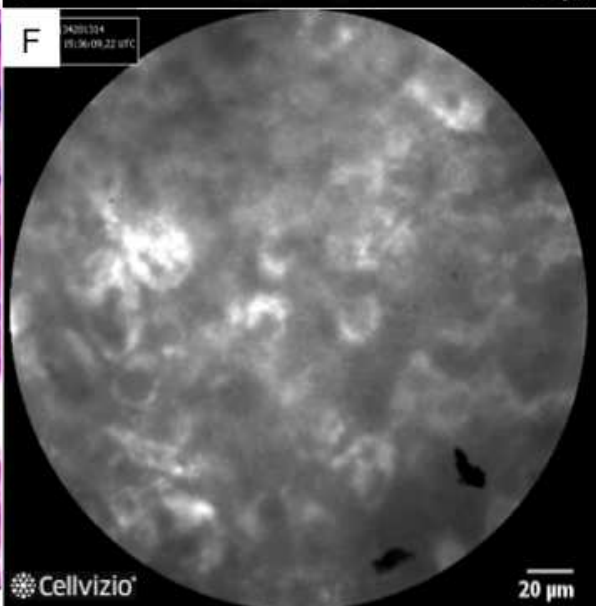
D



E. Acquired Cystic RCC



F



Key of Definitions for Abbreviations

CLE = Confocal laser endomicroscopy
MCT = Monocarboxylic acid transporter
RCC = Renal cell carcinoma
SRM = Small renal mass